



## Magnetic moments of light nuclei from lattice quantum chromodynamics

S.R. Beane,<sup>1</sup> E. Chang,<sup>1,2</sup> S. Cohen,<sup>1,2</sup> W. Detmold,<sup>3</sup> H.W. Lin,<sup>1</sup>  
K. Orginos,<sup>4,5</sup> A. Parreño,<sup>6</sup> M.J. Savage,<sup>1,2</sup> and B.C. Tiburzi<sup>7,8,9</sup>

(NPLQCD Collaboration)

<sup>1</sup>*Department of Physics, University of Washington, Box 351560, Seattle, WA 98195, USA*

<sup>2</sup>*Institute for Nuclear Theory, Box 351550, Seattle, WA 98195-1550, USA*

<sup>3</sup>*Center for Theoretical Physics, Massachusetts Institute of Technology, Cambridge, MA 02139, USA*

<sup>4</sup>*Department of Physics, College of William and Mary, Williamsburg, VA 23187-8795, USA*

<sup>5</sup>*Jefferson Laboratory, 12000 Jefferson Avenue, Newport News, VA 23606, USA*

<sup>6</sup>*Dept. d'Estructura i Constituents de la Matèria. Institut de Ciències del Cosmos (ICC),  
Universitat de Barcelona, Martí Franquès 1, E08028-Spain*

<sup>7</sup>*Department of Physics, The City College of New York, New York, NY 10031, USA*

<sup>8</sup>*Graduate School and University Center, The City University of New York, New York, NY 10016, USA*

<sup>9</sup>*RIKEN BNL Research Center, Brookhaven National Laboratory, Upton, NY 11973, USA*

(Dated: February 25, 2015)

We present the results of lattice QCD calculations of the magnetic moments of the lightest nuclei, the deuteron, the triton and  ${}^3\text{He}$ , along with those of the neutron and proton. These calculations, performed at quark masses corresponding to  $m_\pi \sim 800$  MeV, reveal that the structure of these nuclei at unphysically heavy quark masses closely resembles that at the physical quark masses. In particular, we find that the magnetic moment of  ${}^3\text{He}$  differs only slightly from that of a free neutron, as is the case in nature, indicating that the shell-model configuration of two spin-paired protons and a valence neutron captures its dominant structure. Similarly a shell-model-like moment is found for the triton,  $\mu_{3\text{H}} \sim \mu_p$ . The deuteron magnetic moment is found to be equal to the nucleon isoscalar moment within the uncertainties of the calculations. Furthermore, deviations from the Schmidt limits are also found to be similar to those in nature for these nuclei. These findings suggest that at least some nuclei at these unphysical quark masses are describable by a phenomenological nuclear shell-model.

The electromagnetic interactions of nuclei have been used extensively to elucidate their structure and dynamics. In the early days of nuclear physics, the magnetic moments of the light nuclei helped to reveal that they behaved like a collection of “weakly” interacting nucleons that, to a very large degree, retained their identity, despite being bound together by the strong nuclear force. This feature, in part, led to the establishment of the nuclear shell model as a phenomenological tool with which to predict basic properties of nuclei throughout the periodic table. The success of the shell model is somewhat remarkable, given that nuclei are fundamentally bound states of quarks and gluons, the degrees of freedom of quantum chromodynamics (QCD). The strong nuclear force emerges from QCD as a by-product of confinement and chiral symmetry breaking. The fact that, at the physical values of the quark masses, nuclei are not simply collections of quarks and gluons, defined by their global quantum numbers, but have the structure of interacting protons and neutrons, remains to be understood at a deep level. In this letter, we continue our exploration of nuclei at unphysical quark masses, and calculate the magnetic moments of the lightest few nuclei using lattice QCD. We find that they are close to those found in na-

ture, and also close to the sum of the constituent nucleon magnetic moments in the simplest shell model configuration. This second finding in particular is remarkable and suggests that a phenomenological nuclear shell-model is applicable for at least some nuclei at these unphysical quark masses.

Our lattice QCD calculations were performed on one ensemble of gauge-field configurations generated with a  $N_f = 3$  clover-improved fermion action [1] and a Lüscher-Weisz gauge action [2]. The configurations have  $L = 32$  lattice sites in each spatial direction,  $T = 48$  sites in the temporal direction, and a lattice spacing of  $a \sim 0.12$  fm. All three light-quark masses were set equal to that of the physical strange quark, producing a pion of mass  $m_\pi \sim 806$  MeV. A background electromagnetic ( $U_Q(1)$ ) gauge field giving rise to a uniform magnetic field along the  $z$ -axis was multiplied onto each QCD gauge field in the ensemble (separately for each quark flavor), and these combined gauge fields were used to calculate up- and down-quark propagators, which were then contracted to form the requisite nuclear correlation functions using the techniques of Ref. [3]. Calculations were performed on  $\sim 750$  gauge-field configurations, taken at uniform intervals from  $\sim 10,000$  trajectories. On each configuration,

quark propagators were generated from 48 uniformly distributed Gaussian-smearing sources for each of four magnetic field strengths (for further details of the production, see Refs. [4, 5]).

Background electromagnetic fields have been used extensively to calculate electromagnetic properties of single hadrons, such as the magnetic moments of the lowest-lying baryons [6–14] and electromagnetic polarizabilities of mesons and baryons [9, 12–17]. In order that the quark fields, with electric charges  $Q_u = +\frac{2}{3}$  and  $Q_{d,s} = -\frac{1}{3}$  for the up-, down- and strange-quarks, respectively, satisfy spatially-periodic boundary conditions in the presence of a background magnetic field, it is well-known [18] that the lattice links,  $U_\mu(x)$ , associated with the  $U_Q(1)$  gauge field are of the form

$$U_\mu(x) = e^{i\frac{6\pi Q_q \tilde{n}}{L^2} x_1 \delta_{\mu,2}} \times e^{-i\frac{6\pi Q_q \tilde{n}}{L} x_2 \delta_{\mu,1} \delta_{x_1, L-1}} , \quad (1)$$

for quark of flavour  $q$ , where  $\tilde{n}$  must be an integer. The uniform magnetic field,  $\mathbf{B}$ , resulting from these links is

$$e\mathbf{B} = \frac{6\pi\tilde{n}}{L^2} \hat{\mathbf{z}} , \quad (2)$$

where  $e$  is the magnitude of the electric charge and  $\hat{\mathbf{z}}$  is a unit vector in the  $x_3$ -direction. In physical units, the background magnetic fields exploited with this ensemble of gauge-field configurations are  $e|\mathbf{B}| \sim 0.046 |\tilde{n}| \text{ GeV}^2$ . To optimize the re-use of light-quark propagators in the production, calculations were performed for  $U_Q(1)$  fields with  $\tilde{n} = 0, 1, -2, +4$ . Four field strengths were found to be sufficient for this initial investigation. With three degenerate flavors of light quarks, and a traceless electric-charge matrix, there are no contributions from coupling of the  $\mathbf{B}$  field to sea quarks at leading order in the electric charge. Therefore, the magnetic moments presented here are complete calculations (there are no missing disconnected contributions).

The ground-state energy of a non-relativistic hadron of mass  $M$ , and charge  $Qe$  in a uniform magnetic field is

$$E(\mathbf{B}) = M + \frac{|Qe\mathbf{B}|}{2M} - \boldsymbol{\mu} \cdot \mathbf{B} - 2\pi\beta_{M0} |\mathbf{B}|^2 - 2\pi\beta_{M2} T_{ij} B_i B_j + \dots , \quad (3)$$

where the ellipses denote terms that are cubic and higher in the magnetic field, as well as terms that are  $1/M$  suppressed [19, 20]. The first contribution in eq. (3) is the hadron's rest mass, the second is the energy of the lowest-lying Landau level, the third is from the interaction of its magnetic moment,  $\boldsymbol{\mu}$ , and the fourth and fifth terms are from its scalar and quadrupole magnetic polarizabilities,  $\beta_{M0, M2}$ , respectively ( $T_{ij}$  is a traceless symmetric tensor [21]). The magnetic moment term is only present for particles with spin, and  $\beta_{M2}$  is only present for  $j \geq 1$ . In order to determine  $\boldsymbol{\mu}$  using lattice QCD calculations, two-point correlation functions associated with the hadron or nucleus of interest in the  $j_z = \pm j$

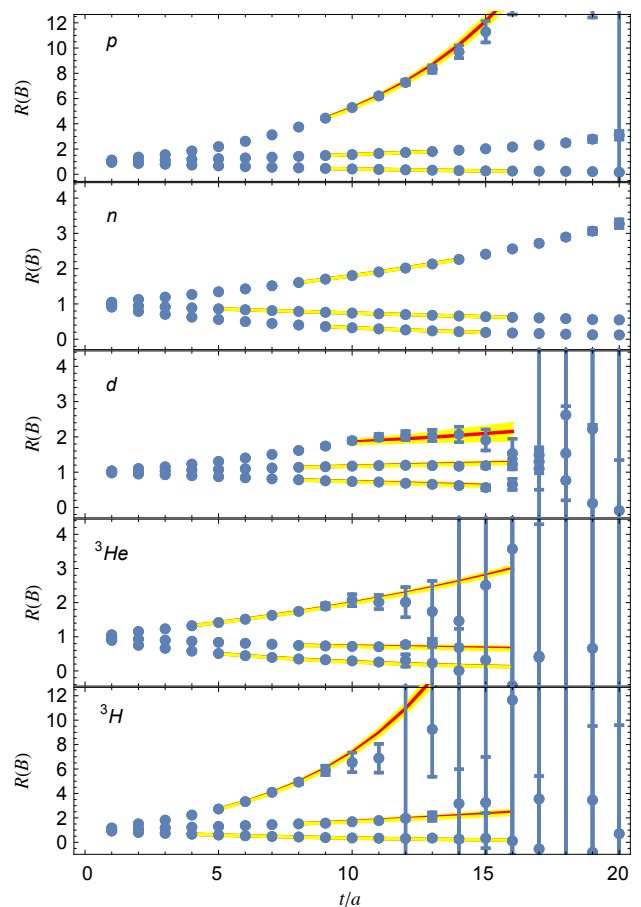


FIG. 1: The correlator ratios  $R(B)$  as a function of time slice for the various states ( $p$ ,  $n$ ,  $d$ ,  ${}^3\text{He}$ , and  ${}^3\text{H}$ ) for  $\tilde{n} = +1, -2, +4$ . Fits to the ratios are also shown.

magnetic sub-states,  $C_{j_z}^{(B)}(t)$ , can be calculated in the presence of background fields of the form given in Eq. (1) with strength  $B = \hat{\mathbf{z}} \cdot \mathbf{B}$ . The energies of ground-states aligned and anti-aligned with the magnetic field,  $E_{\pm j}^B$ , will be split by spin-dependent interactions, and the difference,  $\delta E^{(B)} = E_{+j}^B - E_{-j}^B$ , can be extracted from the correlation functions that we consider. The component of  $\delta E^{(B)}$  that is linear in  $\mathbf{B}$  determines  $\boldsymbol{\mu}$  via Eq. (3). Explicitly, the energy difference is determined from the large time behaviour of

$$R(B) = \frac{C_j^{(B)}(t) C_{-j}^{(0)}(t)}{C_{-j}^{(B)}(t) C_j^{(0)}(t)} \xrightarrow{t \rightarrow \infty} Z e^{-\delta E^{(B)} t} . \quad (4)$$

Each term in this ratio is a correlation function with the quantum numbers of the nuclear state that is being considered, which we compute using the methods of Ref. [3]. As discussed in Ref. [14], subtracting the contribution from the correlation functions calculated in the absence of a magnetic field reduces fluctuations in the ratio, enabling a more precise determination of the magnetic mo-

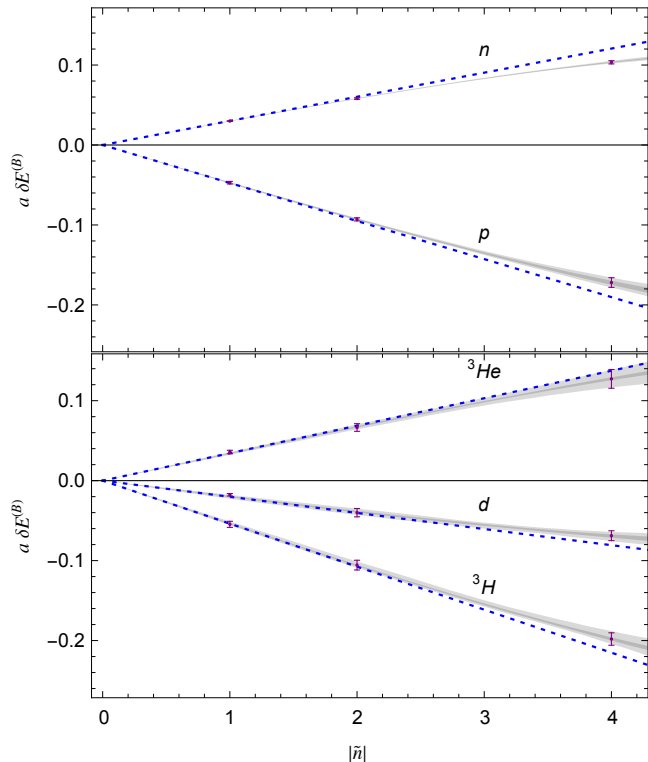


FIG. 2: The calculated  $\delta E^{(B)}$  of the proton and neutron (upper panel) and light nuclei (lower panel) in lattice units as a function of  $|\tilde{n}|$ . The shaded regions corresponds to fits of the form  $\delta E^{(B)} = -2\mu |\mathbf{B}| + \gamma |\mathbf{B}|^3$  and their uncertainties. The dashed lines correspond to the linear contribution alone.

ment. The energy splitting is extracted from a correlated  $\chi^2$ -minimization of the functional form in Eq. (4) using a covariance matrix generated with the jackknife procedure. Fits are performed only over time ranges where all of the individual correlators in the ratio exhibit single exponential behavior and a systematic uncertainty is assigned from variation of the fitting window. Figure 1 shows the correlator ratios and associated fits for the various states that we consider:  $p$ ,  $n$ ,  $d$ ,  ${}^3\text{He}$ , and  ${}^3\text{H}$ , for  $\tilde{n} = +1, -2, +4$ .

As mentioned above, the magnetic moments of the proton and neutron have been previously calculated with lattice QCD methods for a wide range of light-quark masses (in almost all cases omitting the disconnected contributions). The present work is the first QCD calculation of the magnetic moments of nuclei. In Figure 2, we show the energy splittings of the nucleons and nuclei as a function of  $|\tilde{n}|$ , and, motivated by Eq. (3), we fit these to a function of the form  $\delta E^{(B)} = -2\mu |\mathbf{B}| + \gamma |\mathbf{B}|^3$ , where  $\gamma$  is a constant encapsulating higher-order terms in the expansion. We find that the proton and neutron magnetic moments at this pion mass are  $\mu_p = 1.792(19)(37)$  NM (nuclear magnetons) and  $\mu_n = -1.138(03)(10)$  NM, respec-

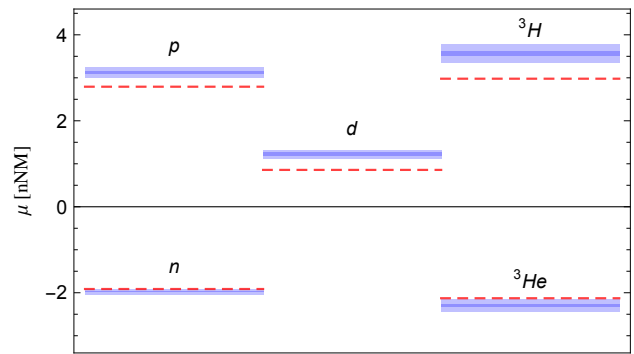


FIG. 3: The magnetic moments of the proton, neutron, deuteron,  ${}^3\text{He}$  and triton. The results of the lattice QCD calculation at a pion mass of  $m_\pi \sim 806$  MeV, in units of natural nuclear magnetons ( $e/2M_N^{\text{latt}}$ ), are shown as the solid bands. The inner bands corresponds to the statistical uncertainties, while the outer bands correspond to the statistical and systematic uncertainties combined in quadrature, and include our estimates of the uncertainties from lattice spacing and volume. The red dashed lines show the experimentally measured values at the physical quark masses.

tively, where the first uncertainty is statistical and the second uncertainty is from systematics associated with the fits to correlation functions and the extraction of the magnetic moment using the above form. These results agree with previous calculations [14] within the uncertainties. The natural units of the system are  $e/2M_N^{\text{latt}}$ , where  $M_N^{\text{latt}}$  is the mass of the nucleon at the quark masses of the lattice calculation, which we refer to as natural nuclear magnetons (nNM). In these units, the magnetic moments are  $\mu_p = 3.119(33)(64)$  nNM and  $\mu_n = -1.981(05)(18)$  nNM. These values at this unphysical pion mass can be compared with those of nature,  $\mu_p^{\text{expt}} = 2.792847356(23)$  NM and  $\mu_n^{\text{expt}} = -1.9130427(05)$  NM, which are remarkably close to the lattice results. In fact, when comparing all available lattice QCD results for the nucleon magnetic moments in units of nNM, the dependence upon the light-quark masses is surprisingly small, reminiscent of the almost completely flat pion mass dependence of the nucleon axial coupling,  $g_A$ .

In Figure 2, we also show  $\delta E^{(B)}$  as a function of  $|\tilde{n}|$  for the deuteron,  ${}^3\text{He}$  and the triton ( ${}^3\text{H}$ ). Fitting the energy splittings with a form analogous to that for the nucleons gives magnetic moments of  $\mu_d = 1.218(38)(87)$  nNM for the deuteron,  $\mu_{{}^3\text{He}} = -2.29(03)(12)$  nNM for  ${}^3\text{He}$  and  $\mu_{{}^3\text{H}} = 3.56(05)(18)$  nNM for the triton. These can be compared with the experimental values of  $\mu_d^{\text{expt}} = 0.8574382308(72)$  NM,  $\mu_{{}^3\text{He}}^{\text{expt}} = -2.127625306(25)$  NM and  $\mu_{{}^3\text{H}}^{\text{expt}} = 2.978962448(38)$  NM. The magnetic moments calculated with lattice QCD, along with their experimental values, are presented in Figure 3. The naive shell-model predictions for the magnetic moments of these light nuclei are  $\mu_d^{\text{SM}} = \mu_p + \mu_n$ ,  $\mu_{{}^3\text{He}}^{\text{SM}} = \mu_n$  (where

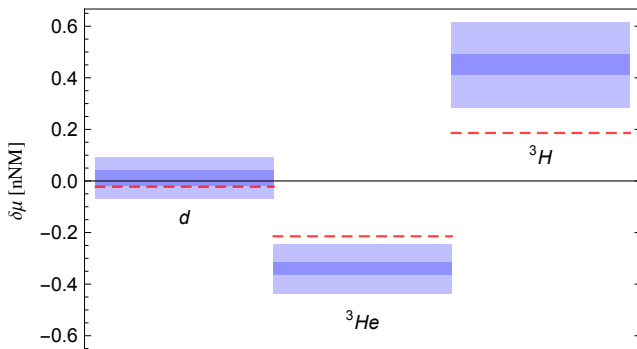


FIG. 4: The differences between the nuclear magnetic moments and the predictions of the naive shell-model. The results of the lattice QCD calculation at a pion mass of  $m_\pi \sim 806$  MeV, in units of natural nuclear magnetons ( $e/2M_N^{\text{latt}}$ ), are shown as the solid bands. The inner band corresponds to the statistical uncertainties, while the outer bands correspond to the statistical and systematic uncertainties combined in quadrature, including estimates of the uncertainties from lattice spacing and volume. The red dashed lines show the experimentally measured differences.

the two protons in the 1s-state are spin paired to  $j_p = 0$  and the neutron is in the 1s-state) and  $\mu_{3\text{H}}^{\text{SM}} = \mu_p$  (where the two neutrons in the 1s-state are spin paired to  $j_n = 0$  and the proton is in the 1s-state). For these simple s-shell nuclei, the proton and neutron magnetic moments correspond to the Schmidt limits [22]. In nature,  ${}^3\text{He}$  is one of the very few nuclei that lie outside the Schmidt limits [23]. In our calculations we also find that  ${}^3\text{He}$  lies outside the Schmidt limits at this heavier pion mass, with  $\delta\mu_{3\text{He}} = \mu_{3\text{He}} - \mu_n = -0.340(24)(93)$  nNM (compared to the experimental difference of  $\delta\mu_{3\text{He}}^{\text{expt}} = -0.215$  NM), and similarly for the triton  $\delta\mu_{3\text{H}} = \mu_{3\text{H}} - \mu_p = +0.45(04)(16)$  nNM (compared to the experimental difference of  $\delta\mu_{3\text{H}}^{\text{expt}} = +0.186$  NM), corresponding to  $\sim 10\%$  deviations from the naive shell-model predictions. These quantities are summarized in Figure 4.

At a phenomenological level, it is not difficult to understand why the magnetic moments scale, to a large degree, with the nucleon mass. The success of the non-relativistic quark model (NRQM) in describing the magnetic moments of the lowest-lying baryons as the sum of contributions from three weakly-bound non-relativistic quarks, with up- and down-quark masses of  $M_{U,D} \sim 300$  MeV and strange-quark mass of  $M_S \sim 500$  MeV, suggests that naive scaling with the hadron mass should capture most of the quark-mass dependence. From the perspective of chiral perturbation theory ( $\chi\text{PT}$ ), the leading contributions to the nucleon magnetic moments are from dimension-five operators, with the leading quark-mass dependence arising from mesons loops that are suppressed in the chiral expansion, and scaling linearly with the mass of the pion. Consistency of the magnetic mo-

ments calculated in the NRQM and in  $\chi\text{PT}$  suggests that the nucleon mass scales linearly with the pion mass, which is inconsistent with chiral power counting, but consistent with the results obtained from analysis of lattice QCD calculations [24]. It should be emphasized that the magnetic moments of the light nuclei that we study here are well understood in the context of nuclear chiral effective field theory, where pions and nucleons are the effective degrees of freedom, and heavier meson-exchange-type contributions are included as various contact interactions among nucleons (see, for instance, Ref. [25]).

The present calculations have been performed at a single lattice spacing and in one lattice volume, and the lack of continuum and infinite volume extrapolations introduces systematic uncertainties into our results. Chiral perturbation theory can be used to estimate the finite volume (FV) effects in the magnetic moments, using the sum of the known [26] effects on the constituent nucleons. These contributions are  $\lesssim 1\%$  in all cases. There may be additional effects beyond the single particle contributions, however the binding energies of light nuclei calculated previously in multiple volumes at this quark mass [4] demonstrate that the current lattice volume is large enough for such FV effects to be negligible. In contrast, calculations with multiple lattice spacings have not been performed at this heavier pion mass, and consequently this systematic uncertainty remains to be quantified. However, electromagnetic contributions to the action are perturbatively improved as they are included as a background field in the link variables. Consequently, the lattice spacing artifacts are expected to be small, entering at  $\mathcal{O}(\Lambda_{\text{QCD}}^2 a^2) \sim 3\%$  for  $\Lambda_{\text{QCD}} = 300$  MeV. To account for these effects, we combine the two sources of uncertainty in quadrature and assess an overall multiplicative systematic uncertainty of 3% on all the extracted moments. For the nuclei, this is small compared to the other systematic uncertainties, but for the neutron in particular, it is the dominant uncertainty.

In conclusion, we have presented the results of lattice QCD calculations of the magnetic moments of the lightest nuclei at the flavor SU(3) symmetric point. We find that, when rescaled by the mass of the nucleon, the magnetic moments of the proton, neutron, deuteron,  ${}^3\text{He}$  and triton are remarkably close to their experimental values. The magnetic moment of  ${}^3\text{He}$  is very close to that of a free neutron, consistent with the two protons in the 1s-state spin-paired to  $j_p = 0$  and the valence neutron in the 1s-state. Analogous results are found for the triton, and the magnetic moment of the deuteron is consistent with the sum of the neutron and proton magnetic moments. This work demonstrates for the first time that QCD can be used to calculate the structure of nuclei from first principles. Calculations using these techniques at lighter quark masses and for larger nuclei are ongoing and will be reported in future work. Perhaps even more importantly, these results reveal aspects of the nature of nuclei,

not at the physical quark masses, but in a more general setting where Standard Model parameters are allowed to vary. In particular, they indicate that the phenomenological successes of the nuclear shell-model in nature may extend over a broad range of quark masses.

We thank D.B. Kaplan and D.R. Phillips for helpful discussions. SRB was supported in part by NSF continuing grant PHY1206498, MJS was supported in part by DOE grant No. DE-FG02-00ER41132, WD was supported by the U.S. Department of Energy Early Career Research Award DE-SC0010495 and the Solomon Buchsbaum Fund at MIT. KO was supported by the U.S. Department of Energy through Grant Number DE-FG02-04ER41302 and through Grant Number DE-AC05-06OR23177 under which JSA operates the Thomas Jefferson National Accelerator Facility. HWL was supported by DOE grant No. DE-FG02-97ER4014. The work of AP was supported by the contract FIS2011-24154 from MEC (Spain) and FEDER. BCT was supported in part by a joint City College of New York–RIKEN/Brookhaven Research Center fellowship, a grant from the Professional Staff Congress of the CUNY, and by the U.S. National Science Foundation, under Grant No. PHY12-05778. This work made use of high-performance computing resources provided by XSEDE (supported by National Science Foundation Grant Number OCI-1053575), NERSC (supported by U.S. Department of Energy Grant Number DE-AC02-05CH11231), the PRACE Research Infrastructure resource Mare Nostrum at the Barcelona SuperComputing Center, and by the USQCD collaboration. Parts of these calculations were performed using the `chroma` lattice field theory library [27].

- 
- [1] B. Sheikholeslami and R. Wohlert, *Nucl.Phys.* **B259**, 572 (1985).  
 [2] M. Lüscher and P. Weisz, *Commun.Math.Phys.* **97**, 59 (1985).

- [3] W. Detmold and K. Orginos, *Phys.Rev.* **D87**, 114512 (2013), 1207.1452.  
 [4] S. Beane, E. Chang, S. Cohen, W. Detmold, H. Lin, et al., *Phys.Rev.* **D87**, 034506 (2013), 1206.5219.  
 [5] S. Beane et al. (NPLQCD Collaboration), *Phys.Rev.* **C88**, 024003 (2013), 1301.5790.  
 [6] C. W. Bernard, T. Draper, K. Olynyk, and M. Rushton, *Phys.Rev.Lett.* **49**, 1076 (1982).  
 [7] G. Martinelli, G. Parisi, R. Petronzio, and F. Rapuano, *Phys.Lett.* **B116**, 434 (1982).  
 [8] F. Lee, R. Kelly, L. Zhou, and W. Wilcox, *Phys.Lett.* **B627**, 71 (2005), hep-lat/0509067.  
 [9] F. X. Lee, L. Zhou, W. Wilcox, and J. C. Christensen, *Phys.Rev.* **D73**, 034503 (2006), hep-lat/0509065.  
 [10] W. Detmold, B. Tiburzi, and A. Walker-Loud, *Phys.Rev.* **D73**, 114505 (2006), hep-lat/0603026.  
 [11] C. Aubin, K. Orginos, V. Pascalutsa, and M. Vanderhaeghen, *Phys.Rev.* **D79**, 051502 (2009), 0811.2440.  
 [12] W. Detmold, B. C. Tiburzi, and A. Walker-Loud, *Phys.Rev.* **D79**, 094505 (2009), 0904.1586.  
 [13] W. Detmold, B. Tiburzi, and A. Walker-Loud, *Phys.Rev.* **D81**, 054502 (2010), 1001.1131.  
 [14] T. Primer, W. Kamleh, D. Leinweber, and M. Burkardt, *Phys.Rev.* **D89**, 034508 (2014), 1307.1509.  
 [15] H. Fiebig, W. Wilcox, and R. Woloshyn, *Nucl.Phys.* **B324**, 47 (1989).  
 [16] J. C. Christensen, W. Wilcox, F. X. Lee, and L.-m. Zhou, *Phys.Rev.* **D72**, 034503 (2005), hep-lat/0408024.  
 [17] M. Lujan, A. Alexandru, W. Freeman, and F. Lee, *Phys.Rev.* **D89**, 074506 (2014), 1402.3025.  
 [18] G. 't Hooft, *Nucl.Phys.* **B153**, 141 (1979).  
 [19] R. J. Hill and G. Paz, *Phys.Rev.Lett.* **107**, 160402 (2011), 1103.4617.  
 [20] J.-W. Lee and B. C. Tiburzi (2014), 1407.8159.  
 [21] J.-W. Chen, H. W. Grieshammer, M. J. Savage, and R. P. Springer, *Nucl.Phys.* **A644**, 221 (1998), nucl-th/9806080.  
 [22] T. Schmidt, *Z. Phys.* **106**, 358 (1937).  
 [23] L. L. Foldy and F. J. Milford, *Phys.Rev.* **80**, 751 (1950).  
 [24] A. Walker-Loud, *PoS* **CD12**, 017 (2013), 1304.6341.  
 [25] M. Piarulli, L. Girlanda, L. Marcucci, S. Pastore, R. Schiavilla, et al., *Phys.Rev.* **C87**, 014006 (2013), 1212.1105.  
 [26] B. C. Tiburzi, *Phys.Rev.* **D89**, 074019 (2014), 1403.0878.  
 [27] R. G. Edwards and B. Joo, *Nucl.Phys.Proc.Suppl.* **140**, 832 (2005), hep-lat/0409003.